



Cite this: *J. Anal. At. Spectrom.*, 2026, **41**, 1928

Determination of absolute isotope ratios of vanadium by internal standardisation

D. Malinovsky, * P. J. H. Dunn, B. A. Engin and H. Goenaga-Infante

Due to the prohibitively high cost of materials enriched in the ^{50}V isotope, internal standardisation is the only viable method for the determination of absolute vanadium isotope ratios by mass spectrometry. This work describes methodology that applies, for the first time, internal standardisation to the determination of $n(^{51}\text{V})/n(^{50}\text{V})$ isotope ratios by multi-collector inductively coupled plasma mass spectrometry (MC-ICP-MS). To achieve this, solutions of vanadium standard NIST SRM 3165 were doped with iron standard IRMM-014 with certified Fe isotope amount ratios, which was used as a calibrant in the measurements. A comparison of the performance of the established models to correct for instrumental mass fractionation showed that although the mean $n(^{51}\text{V})/n(^{50}\text{V})$ values obtained by the regression model and the exponential model were statistically indistinguishable (399.8 ± 12.6 and 397.3 ± 1.7 , U_{expanded} , $k = 2$, respectively), their uncertainties were remarkably different. High uncertainty of the $n(^{51}\text{V})/n(^{50}\text{V})$ value by the regression model was attributed to bias arising due to heterogeneity of variance of measured data on the log scale in a situation when isotope ratios of an analyte and an internal standard are significantly different. By its nature, the regression model offered an important advantage of assumption-free calibration, and, following its unsatisfactory performance, a new calibration method that does not rely on *a priori* assumed functional form of instrumental isotope fractionation was developed in this study. The new method is based on extracting a calibration factor for measured $^{51}\text{V}/^{50}\text{V}$ ratios from the relationship constructed between calibration factors obtained for measured isotope ratios of the internal standard and ratios of relative atomic masses making up these ratios ($^{56}\text{Fe}/^{54}\text{Fe}$, $^{57}\text{Fe}/^{54}\text{Fe}$ and $^{57}\text{Fe}/^{56}\text{Fe}$). The data obtained allowed us to re-determine the atomic weight of vanadium in NIST SRM 3165, to get $A_r(\text{V}) = 50.94146 \pm 0.00003$ (U_{expanded} , $k = 2$), with the uncertainties improved by a factor of four as compared to the last estimate made in 1977.

Received 21st December 2025
 Accepted 10th April 2026

DOI: 10.1039/d5ja00509d

rsc.li/jaas

Introduction

Vanadium has two stable isotopes, namely ^{50}V and ^{51}V , with natural abundances of $\sim 0.25\%$ and $\sim 99.75\%$, respectively. Variations in the abundances of vanadium isotopes were shown to be useful markers in geochemistry and environmental science.^{1–10} They help discriminate the origin of vanadium containing materials and can provide insight into migration pathways of the element. Recent studies documented an increase in global anthropogenic releases of the element to soil and water that led to naming vanadium a re-emerging environmental hazard.¹¹ Given the potential offered by vanadium isotope data in the above areas, further studies employing vanadium isotopes are warranted.

Vanadium isotope ratio data were reported previously almost exclusively as delta values. Despite being a convenient way of reporting results, the delta value notation has an important drawback of poor data comparability in the situation when an

isotope standard used is not certified for absolute isotope ratios. This is precisely the situation for vanadium isotope ratio measurements as there is no vanadium material with certified $n(^{51}\text{V})/n(^{50}\text{V})$ ratios.

The determination of absolute isotope ratios of vanadium with high accuracy and precision is a very non-trivial task. The traditional method for the determination of absolute isotope ratios is based on the use of synthetic isotope mixtures to calibrate measurements. These calibration mixtures need to be prepared from parent materials highly enriched in ^{50}V and ^{51}V isotopes. However, the cost of ^{50}V isotope materials, such as vanadium oxides, with the required degree of enrichment is prohibitively high, starting from more than five thousand US dollars for a milligram of vanadium pentoxide enriched in ^{50}V isotope.¹²

An alternative calibration method is internal standardisation. Using this approach, an internal standard with a known amount of a substance, different from the analyte of interest, is added to samples to correct for fluctuations in instrument response during analysis and as an aid for calibration.^{13,14} It has been shown that normalisation to an internal

National Measurement Laboratory, LGC, 10 Priestley Road, Guildford, GU2 7XY, UK.
 E-mail: dmitriy.malinovskiy@lgcgroup.com



standard with certified isotope abundances by using the so-called regression method is the metrologically rigorous method for the determination of isotope amount ratios.^{15–17} Empirical models based on *a priori* assumed functional relationships between measured isotope ratios of an analyte and internal standard are also a popular choice, albeit it is known that the accuracy of results obtained by these models is often poor.¹⁸

In this study, the performance of the existing approaches for the determination of the $n(^{51}\text{V})/n(^{50}\text{V})$ isotope ratio of vanadium standard solution NIST SRM 3165 by normalisation to the internal standard with certified Fe isotope abundances has been systematically evaluated. Following initial results, a novel method for obtaining a calibration factor that relates true and measured isotope ratios of vanadium was developed and validated. The isotope ratio data obtained using the new method have enabled re-determination of the atomic weight of vanadium with a four-fold improvement in measurement uncertainty relative to the last IUPAC estimate in the year 1977.

Experimental

Materials and reagents

Single element NIST Standard Reference Material 3165, a vanadium standard solution (Lot No. 992706, NIST, USA) certified only for concentration of vanadium, was used as the sample in this study. IRMM-014 Fe solution with certified Fe isotope abundances was used as the internal standard in the measurements (JRC, Belgium). High purity deionised water was obtained using an ELGA water purification system (Veolia Water, Marlow, UK). Ultrapure nitric acid was purchased from Romil (Cambridge, UK) and used as supplied by the manufacturer.

Mass spectrometry and uncertainty estimation

Vanadium and iron isotope ratios were measured by multi-collector ICP-MS (Neptune, Thermo Scientific, Germany). A stable introduction system consisting of a peristaltic pump, a 50 $\mu\text{l min}^{-1}$ microconcentric PFA nebulizer, and a tandem quartz spray chamber arrangement (cyclone + Scott double pass) was

used for sample introduction. $^{50}\text{V}^+$, $^{51}\text{V}^+$, $^{52}\text{Cr}^+$, $^{53}\text{Cr}^+$, $^{54}\text{Fe}^+$, $^{56}\text{Fe}^+$ and $^{57}\text{Fe}^+$ isotopic ions were collected simultaneously in static mode at Low 3, Low 2, Low 1, Central, High 1, High 2 and High 4 Faraday cup positions, respectively. Signals on ^{52}Cr and ^{53}Cr isotopes were monitored in the case of a potential presence of chromium which also has a minor ^{50}Cr isotope which, if present, interferes with the ^{50}V isotope. The least abundant ^{58}Fe isotope was not measured because it was not possible to achieve a well-aligned static Faraday cup configuration that included ^{50}V and ^{58}Fe isotopes due to the limitations on ion beam dispersion in MC-ICP-MS and the fact that an ion counter was installed on the Low 4 Faraday cup.

The NIST SRM 3165 standard solution was in most cases diluted to a vanadium concentration of $\sim 2 \text{ mg l}^{-1}$ and spiked with the IRMM-014 Fe standard at $\sim 2 \text{ mg l}^{-1}$. In the beginning of each measurement session, the instrument was carefully tuned to maximise the intensity of the vanadium signal by adjusting the torch position, gas flow rates, and lens voltages. Typical operating conditions for MC-ICPMS are shown in Table 1. All analyses were conducted in high mass resolution mode of the instrument ($R \sim 9000$). Typical sensitivities for $^{51}\text{V}^+$ and $^{56}\text{Fe}^+$ isotopic ions were ~ 6 volts and ~ 5 volts per mg l^{-1} , respectively.

With the aim of producing a larger extent of variations in instrumental mass bias, the measurement protocol involved a series of single measurements, each with an incremental change in the RF power away from the maximum sensitivity setting at $\sim 1100 \text{ W}$ with steps ranging from 10 W to 40 W.^{16,17} Each measurement consisted of 100 cycles, with each cycle having an 8 second duration. It was always verified in the on-line scan window prior to starting the next measurement that the measurement position was in the middle of the interference-free plateau of the $^{50}\text{V}^+$ and $^{56}\text{Fe}^+$ signals.

Vanadium and iron ion current intensities were corrected for procedural blank. The blank signal on the least abundant ^{50}V isotope was always lower than 0.1% and lower than 0.05% for ^{51}V and all Fe isotopes. $n(^{51}\text{V})/n(^{50}\text{V})$ isotope ratio calculations were performed off-line using a template made in MS Excel program. Combined standard uncertainties of measurement results were obtained by propagating the uncertainty of

Table 1 Typical operating conditions and detector configurations of the MC-ICP-MS

RF power, W	1100						
Sample and skimmer cones	Nickel, 1.1 mm and 0.8 mm orifice diameter, respectively; H-type skimmer cone						
Argon gas flow rate, l min^{-1}	15.4						
Cool/plasma	~ 0.9						
Auxiliary	~ 1.05						
Nebuliser	$\sim 0.10\text{--}0.12$						
Sample uptake rate, ml min^{-1}	~ 9000						
Mass resolution, $R_{(5-95\%)}$	Optimised for maximum intensity of the vanadium signal						
Ion lens settings	~ 6.4						
Typical $^{51}\text{V}^+$ sensitivity, V mg l^{-1}							
Detector configuration							
Isotope m/z	^{50}V	^{51}V	^{52}Cr	^{53}Cr	^{54}Fe	^{56}Fe	^{57}Fe
Faraday cup	L3	L2	L1	Centre	H1	H2	H3
Cup position, mm	74.300	47.100	21.080	0.000	22.540	68.340	90.310



individual components according to the ISO/GUM Guide (see details in the SI).

Results and discussion

Calibration of $n(^{51}\text{V})/n(^{50}\text{V})$ isotope ratios by using the regression model

The regression model is based on correlated temporal drift between simultaneously measured isotope ratios of the analyte element and internal standard element. The rationale of the model was detailed in previous works.^{15–17} It can be shown that when using the $^{56}\text{Fe}/^{54}\text{Fe}$ ratio of isotopically certified iron as the internal standard as a calibrator, mass bias corrected isotope ratios of vanadium, $n(^{51}\text{V})/n(^{50}\text{V})$, can be calculated as follows:

$$R_{^{51}\text{V}/^{50}\text{V}} = e^a \cdot R_{^{56}\text{Fe}/^{54}\text{Fe}}^b \quad (1)$$

where $R_{^{51}\text{V}/^{50}\text{V}}$ is $n(^{51}\text{V})/n(^{50}\text{V})$, the mass bias corrected isotope ratio of vanadium, $R_{^{56}\text{Fe}/^{54}\text{Fe}}$ is the certified $n(^{56}\text{Fe})/n(^{54}\text{Fe})$ ratio of the internal standard, and b and a are the slope and intercept of a linear regression of $\ln(^{51}\text{V}/^{50}\text{V})_{\text{measured}}$ versus $\ln(^{56}\text{V}/^{54}\text{Fe})_{\text{measured}}$, respectively.

A notable advantage of using iron as an internal standard is that the element has four stable isotopes, namely ^{54}Fe , ^{56}Fe , ^{57}Fe , and ^{58}Fe . The abundances of these isotopes were certified in the IRMM-014 isotope standard and allow us to use $^{56}\text{Fe}/^{54}\text{Fe}$, $^{57}\text{Fe}/^{54}\text{Fe}$, and $^{57}\text{Fe}/^{56}\text{Fe}$ isotope ratios to calibrate the measured $^{51}\text{V}/^{50}\text{V}$ ratios of the NIST SRM 3165 material. Therefore, equations analogous to eqn (2) can be written when $^{57}\text{Fe}/^{54}\text{Fe}$ and $^{57}\text{Fe}/^{56}\text{Fe}$ isotope ratios are used for calibration. This also implies that each measurement yields a vanadium isotope ratio that represents a grand mean of three $^{51}\text{V}/^{50}\text{V}$ ratio values calculated by normalisation to $^{56}\text{Fe}/^{54}\text{Fe}$, $^{57}\text{Fe}/^{54}\text{Fe}$, and $^{57}\text{Fe}/^{56}\text{Fe}$ isotope ratios of the admixed internal standard, respectively.

Another point to consider is that the slope and intercept of regression can be calculated by using either an ordinary linear regression (OLR), that does not account for measurement errors in variables X and Y , or an errors-in-variables model that does

account for measurement errors. The use of the latter can help achieve higher accuracy in estimates of slopes and intercepts but often at the cost of higher uncertainties associated with their values. A weighted linear regression (WLR) as described by MacTaggart and Farwell (1992)¹⁹ was used in this work as one of the variants of the errors-in-variables model.

$n(^{51}\text{V})/n(^{50}\text{V})$ isotope ratios obtained by using the regression model in 12 independent measurement sessions are shown in Fig. 1. After examining these data, two observations can be made. First, there is a good agreement between values obtained by OLR and WLR. Second, there is significant dispersion in $n(^{51}\text{V})/n(^{50}\text{V})$ isotope ratios between measurement sessions, resulting in high uncertainty of the grand mean. The OLR approach yields an $n(^{51}\text{V})/n(^{50}\text{V})$ isotope ratio of NIST SRM 3165 equal to 399.8 ± 12.6 ($U_{\text{expanded}}, k = 2$). The WLR approach yields an $n(^{51}\text{V})/n(^{50}\text{V})$ isotope ratio of the same solution equal to 401.9 ± 23 ($U_{\text{expanded}}, k = 2$). In relative terms, these uncertainties are 3.1% and 5.7%, respectively. In comparison to previous studies which used the regression model for calibration of isotope ratios of medium and heavy mass elements, the results obtained for vanadium are poor.

Interestingly, when measured $^{51}\text{V}/^{50}\text{V}$ and $^{56}\text{Fe}/^{54}\text{Fe}$ isotope ratios without mass bias correction are presented with the same statistical treatment as the data in Fig. 1, we can see that they are much more repeatable. As can be seen from Fig. 2, the mean value for all measured $^{51}\text{V}/^{50}\text{V}$ isotope ratios is equal to 408.6 ± 1.0 ($U_{\text{expanded}}, k = 2$), and the mean value for all measured $^{56}\text{Fe}/^{54}\text{Fe}$ isotope ratios is equal to 16.510 ± 0.071 ($U_{\text{expanded}}, k = 2$). In relative terms, these uncertainties are 0.24% and 0.43%, respectively.

Comparison of the data shown in Fig. 1 and 2 reveals that the main reason for poor repeatability of vanadium isotope ratios calibrated by the regression model is the lack of accuracy in the determination of regression parameters. Difficulties in obtaining an accurate slope and intercept of linear regression through V and Fe isotope ratio data plotted in ln–ln space are

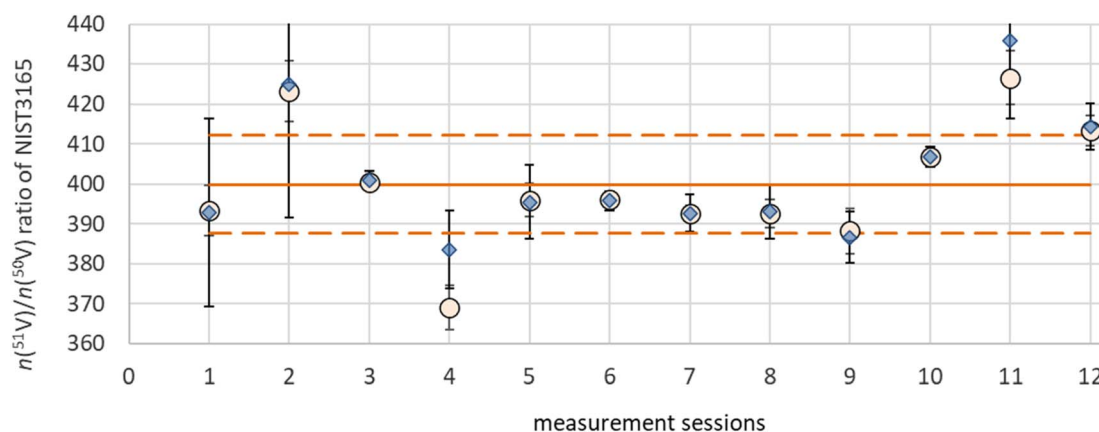


Fig. 1 $n(^{51}\text{V})/n(^{50}\text{V})$ isotope ratios obtained by using the regression model. Filled circles represent the results of Ordinary Linear Regression (OLR). Filled diamonds represent the results of Weighted Linear Regression (WLR). Each data point is the mean of three $^{51}\text{V}/^{50}\text{V}$ isotope ratio values calculated by normalisation to $^{56}\text{Fe}/^{54}\text{Fe}$, $^{57}\text{Fe}/^{54}\text{Fe}$, and $^{57}\text{Fe}/^{56}\text{Fe}$ isotope ratios of the internal standard. Uncertainty bars are combined standard uncertainty. Solid line and dashed lines are the grand mean and expanded uncertainty ($k = 2$) of the results by OLR.



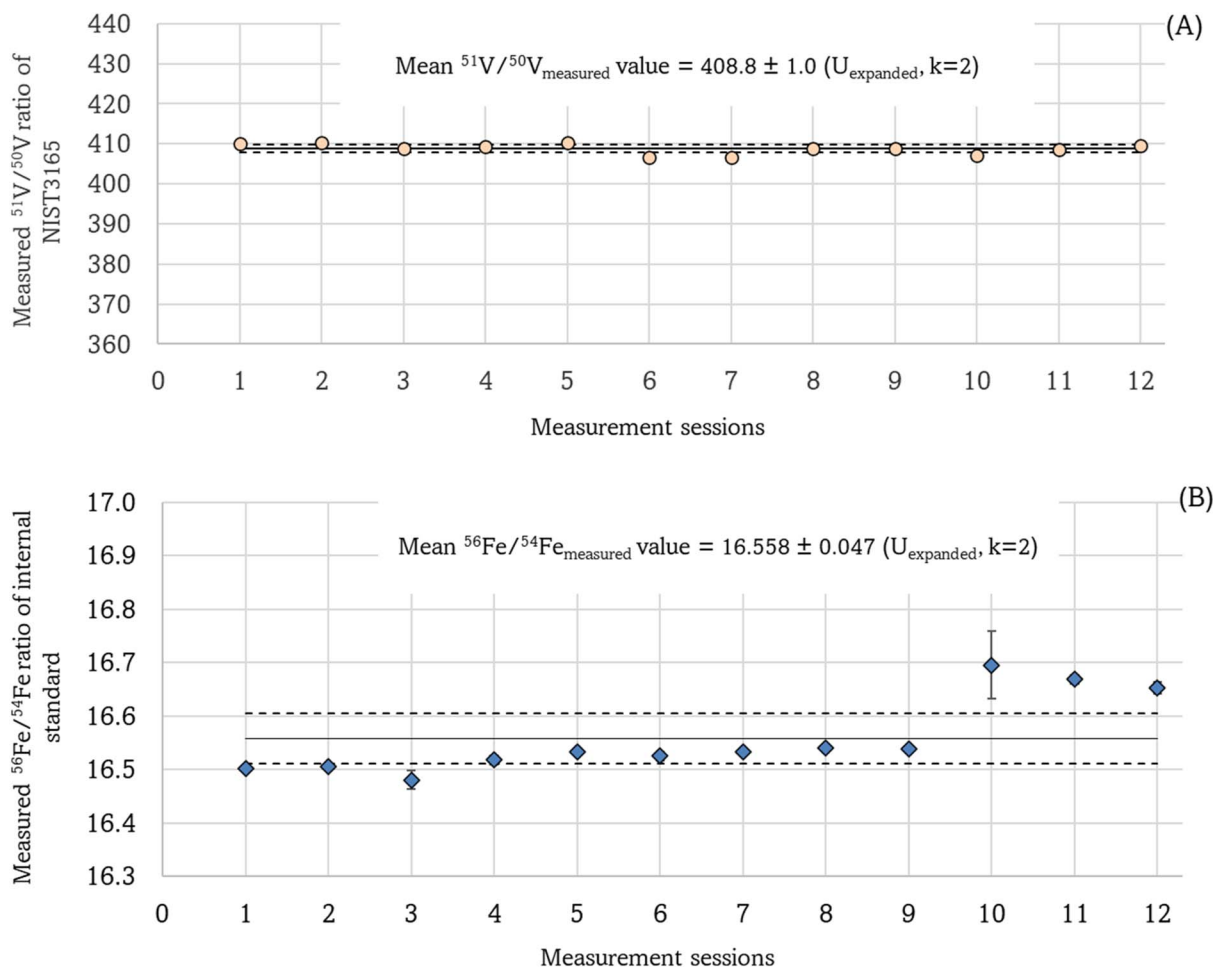


Fig. 2 Variations in measured $^{51}\text{V}/^{50}\text{V}$ and $^{56}\text{Fe}/^{54}\text{Fe}$ isotope ratios in this study, without mass bias correction applied ((A and B), respectively). Each data point is a mean value of replicates in a measurement session. Uncertainty bars are combined standard uncertainty. Solid lines and dashed lines are expanded uncertainties with a coverage factor of 2.

largely driven by the inherent properties of the natural logarithmic function.

A logarithmic curve, defined by the equation $y = \ln(x)$, is characterised by a decreasing rate of change that levels off as the input variable, x , grows (Fig. 3A). As a consequence, the vertical variability in a plot of logarithmic data may depend on where you are on the horizontal scale, with variance of the measurement data in the region of Fe isotope ratios (e.g., $^{56}\text{Fe}/^{54}\text{Fe} \approx 16.5$ and $\ln(^{56}\text{Fe}/^{54}\text{Fe}) \approx 2.8$) being slightly different to variance of the data for a large isotope ratio, such as that of vanadium ($^{51}\text{V}/^{50}\text{V} \approx 408$ and $\ln(^{51}\text{V}/^{50}\text{V}) \approx 6.01$).

This problem of unequal variance, also known as heterogeneity of variance or heteroscedasticity, was discussed previously for the log transformed data as it can lead to bias in estimating regression coefficients.^{20–22} A plot of residuals *versus* predicted values of $\ln(^{51}\text{V}/^{50}\text{V})$ used in identifying heteroscedasticity of the data is shown in Fig. 3B. As can be seen from this figure, the scatter of data points forms a funnel shape pattern which is commonly interpreted as an indicator of unequal variance. More rigorous techniques can be used to confirm heteroscedasticity of the data, including Welch's *t*-test. However, to

obtain strong evidence, one will need to consider a wider than natural range of $\ln(^{51}\text{V}/^{50}\text{V})$ values, which can only be obtained using synthetically prepared synthetic isotope mixtures of enriched vanadium isotopes. Yet, as noted above, the prohibitively high cost of the enriched ^{50}V isotope does not allow easy implementation of such tests.

It is also worth noting that previous studies that determined isotope amount ratios of Ni, Mo, Pb and other elements with high accuracy and precision by using the regression model worked with more favourable ranges of isotope ratios of analytes and internal standards.^{15–17,23–28} When plotted on a \ln - \ln scale, the isotope ratios of analytes and internal standards in these studies were not as significantly different as in the case of vanadium.

Calibration by using the exponential model and robustness of the measurements

The measurement procedure with incremental changes in RF power offers a good opportunity to test the robustness of measurements with internal standardisation. The robustness or ruggedness of an analytical method means its capacity to remain unaffected by small variations in the operating



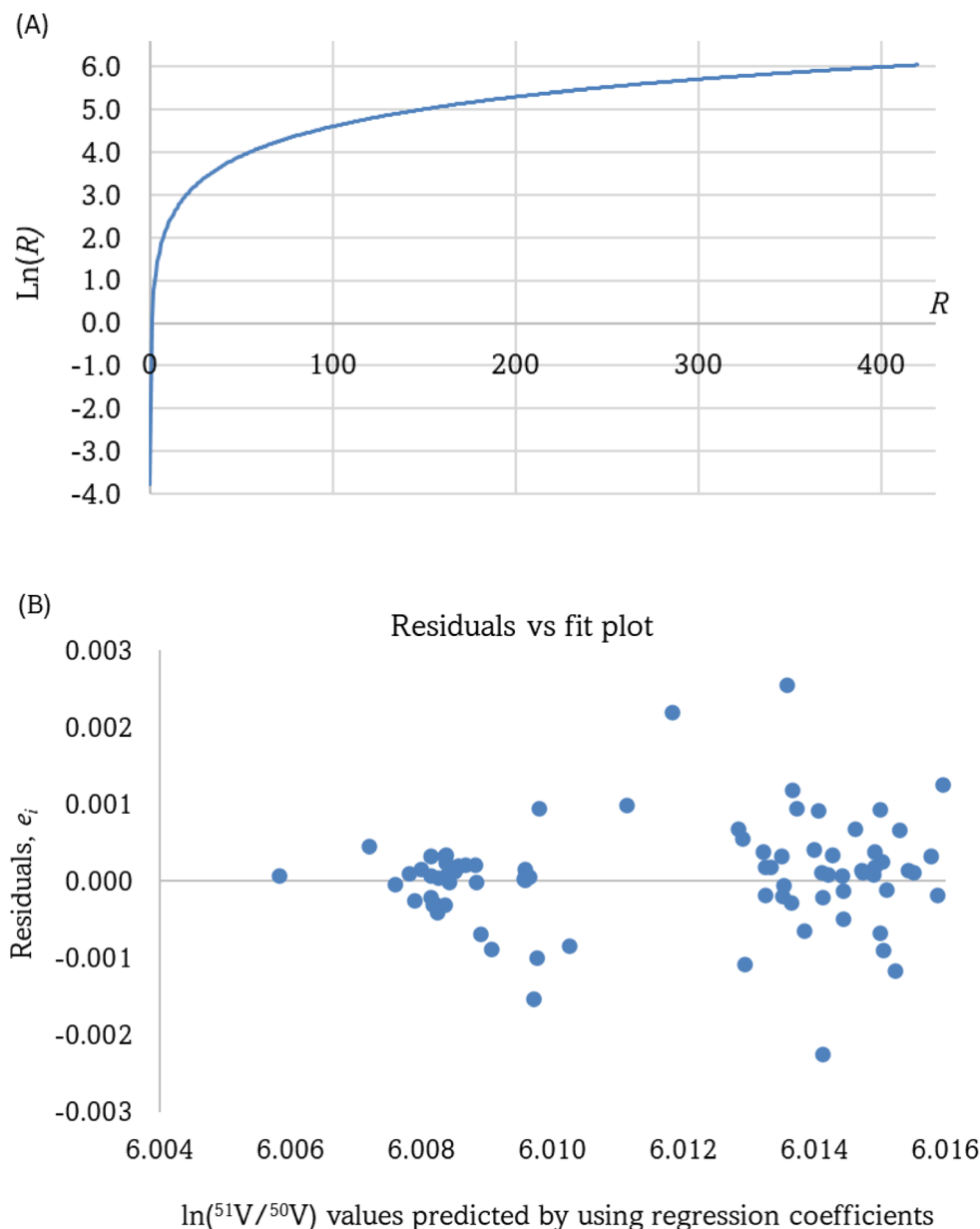


Fig. 3 An illustration of a potential cause for unequal variance of the log transformed Fe and V isotope ratios. Part (A): the natural logarithmic function, corresponding to the range of isotope ratios from 0.023 to 411 considered in this study, is a non-linear curve. The rate of change in the Y axis values of this curve is dependent on the position on the horizontal scale. Part (B): a plot of residuals vs. fit values for all measurements of $^{51}\text{V}/^{50}\text{V}$ ratios made in this study. The vertical distance between any one measured data point, y_i , and its value, \hat{y}_i , predicted by using regression coefficients is known as "residual": $e_i = y_i - \hat{y}_i$. A funnel like pattern of the data on such plots is commonly interpreted as an indicator of unequal variance²¹ (see the text for details).

parameters and produce consistent and repeatable results.²⁹ The exponential model is well suited for testing the repeatability of results obtained under slightly changed measurement conditions because the calibration factor can be calculated from a single measurement of isotope ratios of an analyte and an internal standard.

Mass bias corrected vanadium isotope ratios were calculated using the approach by Russell *et al.* (1978),^{18,30} written as follows in the case of the $^{56}\text{Fe}/^{54}\text{Fe}$ ratio of the internal standard:

$$R_{^{51}\text{V}/^{50}\text{V}} = K \cdot r_{^{51}\text{V}/^{50}\text{V}} \quad (2)$$

$$K = \left(\frac{A_r(^{51}\text{V})}{A_r(^{50}\text{V})} \right)^f \quad (3)$$

$$f = \frac{\ln\left(\frac{R_{^{56}\text{Fe}/^{54}\text{Fe}}}{r_{^{56}\text{Fe}/^{54}\text{Fe}}}\right)}{\ln\left(\frac{A_r(^{56}\text{Fe})}{A_r(^{54}\text{Fe})}\right)} \quad (4)$$

where $R_{^{51}\text{V}/^{50}\text{V}}$ is the vanadium isotope ratio corrected for instrumental mass bias; K is the calibration factor to correct for instrumental mass bias of vanadium isotopes; f is the



exponential model mass fractionation coefficient; $r_{^{51}\text{V}/^{50}\text{V}}$ is the measured vanadium isotope ratio; $R_{^{56}\text{Fe}/^{54}\text{Fe}}$ is the certified Fe isotope ratio; $r_{^{56}\text{Fe}/^{54}\text{Fe}}$ is the measured Fe isotope ratio; and $\text{Ar}(^{50}\text{V})$, $\text{Ar}(^{51}\text{V})$, $\text{Ar}(^{54}\text{Fe})$ and $\text{Ar}(^{56}\text{Fe})$ are the relative atomic masses of vanadium and iron isotopes.

The $n(^{51}\text{V})/n(^{50}\text{V})$ isotope ratios of NIST SRM 3165 obtained by using the exponential model are shown in Fig. 4. These ratios are very reproducible, with the grand mean of 397.3 ± 1.7 (U_{expanded} , $k = 2$). In relative terms, the expanded uncertainty of the result obtained by the exponential model is equal to 0.42% and that is much lower than the expanded uncertainties of the results of the regression model discussed above.

New method of calibration using internal standardisation

The new method exploits the fact that three isotope ratios of the internal standard, namely $^{56}\text{Fe}/^{54}\text{Fe}$, $^{57}\text{Fe}/^{54}\text{Fe}$ and $^{57}\text{Fe}/^{56}\text{Fe}$, were measured simultaneously with the $^{51}\text{V}/^{50}\text{V}$ isotope ratio. Since Fe isotope abundances in the internal standard were certified, it is possible to construct a relationship between calibration factors obtained using the isotope ratios of the internal standard and ratios of relative atomic masses of ^{54}Fe , ^{56}Fe , and ^{57}Fe isotopes, making up these ratios. Fig. 5 shows such a relationship based on the results of a single measurement session. This relationship can be plotted on both a linear scale and a ln–ln scale. The lines passing through the data points in Fig. 5 closely approximate the distribution of calibration factors as a function of relative atomic mass ratios over the narrow range of values defined by Fe isotopes.

At the same time, the relative atomic mass ratio of ^{51}V and ^{50}V isotopes, that is equal to 1.020, sits within the range defined by the relative atomic mass ratios of Fe isotopes. A calibration factor for the measured $^{51}\text{V}/^{50}\text{V}$ isotope ratio can therefore be calculated using parameters of regression through the data obtained for the internal standard. The $n(^{51}\text{V})/n(^{50}\text{V})$ isotope ratios obtained by this approach, with extracting calibration factors from the Fe isotope data plotted on a linear scale, are

shown in Fig. 6. The grand mean value of these $n(^{51}\text{V})/n(^{50}\text{V})$ isotope ratios is 397.59 ± 2.04 (U_{expanded} , $k = 2$). A nearly identical grand mean value of 397.60 ± 2.04 (U_{expanded} , $k = 2$) was obtained when calibration factors for vanadium isotope ratios were extracted from the Fe isotope data plotted on a ln–ln scale.

The combined standard uncertainties of $n(^{51}\text{V})/n(^{50}\text{V})$ isotope ratios were estimated by propagating uncertainty through the calculations with the aid of the numerical method of differentiation by Kragten (1994).³¹ The largest contribution to total uncertainty budget of the new method comes from uncertainty in determining the K factor from Fe isotope ratios of the internal standard that, on average, accounts for 70% of total uncertainty. Contribution from measurements of the analyte, $^{51}\text{V}/^{50}\text{V}$ isotope ratio, accounts for the remaining 30% of total uncertainty.

To compare the results of the new calibration method with results of the exponential and regression models, the $n(^{51}\text{V})/n(^{50}\text{V})$ isotope ratio values of NIST SRM 3165 and their uncertainties obtained in this study are shown in Fig. 7. As can be seen from this figure, the result of the new method is in excellent agreement with the result of the exponential model. A closer look at the procedure by which the abundances of Fe isotopes were determined in the standard IRMM-014 reveals why this agreement is so good. Only the $n(^{56}\text{Fe})/n(^{54}\text{Fe})$ isotope ratio of the IRMM-014 standard was calibrated using the gravimetrically prepared mixtures of enriched ^{56}Fe and ^{54}Fe isotopes; other isotope ratios were obtained using an internal normalisation procedure.³² This implies that once an internal standard with independently calibrated Fe isotope ratios is used, the accuracy of $n(^{51}\text{V})/n(^{50}\text{V})$ isotope ratio measurements by the new method can further be improved. Likewise, uncertainties of the measurements can also be improved provided that isotope amount ratios of a new Fe isotope standard have lower uncertainties than those of the IRMM-014 material.

It is also worth noting that calculating a calibration factor for measured vanadium isotope ratios from the relationship between calibration factors and relative atomic mass ratios of

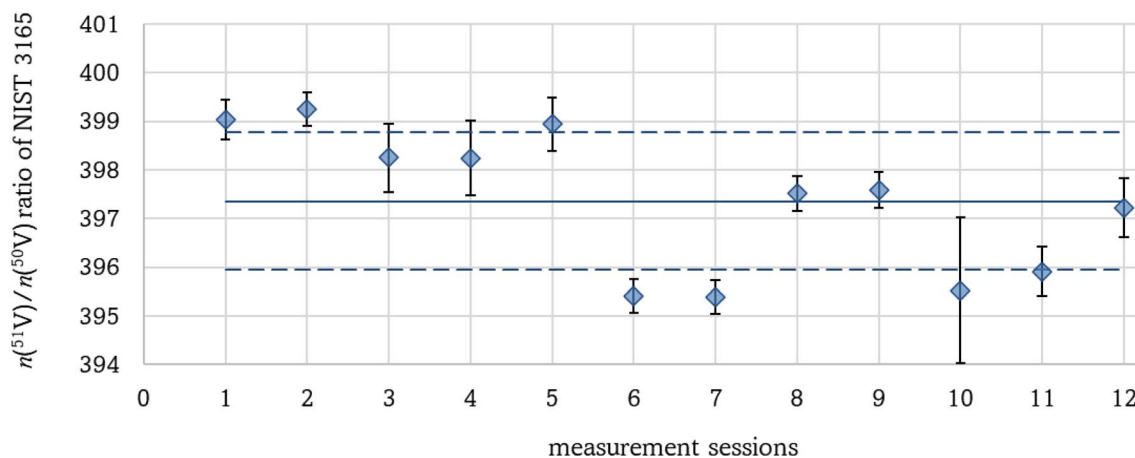


Fig. 4 $n(^{51}\text{V})/n(^{50}\text{V})$ isotope ratios obtained by using the exponential model. Each data point is the mean of three $^{51}\text{V}/^{50}\text{V}$ isotope ratio values calculated by normalisation to $^{56}\text{Fe}/^{54}\text{Fe}$, $^{57}\text{Fe}/^{54}\text{Fe}$, and $^{57}\text{Fe}/^{56}\text{Fe}$ isotope ratios of the internal standard in a measurement session. Uncertainty bars are combined standard uncertainty. Solid line and dashed lines are the grand mean and expanded uncertainty ($k = 2$) of the results. Mean value is equal to 397.4 ± 1.4 (U_{expanded} , $k = 2$).



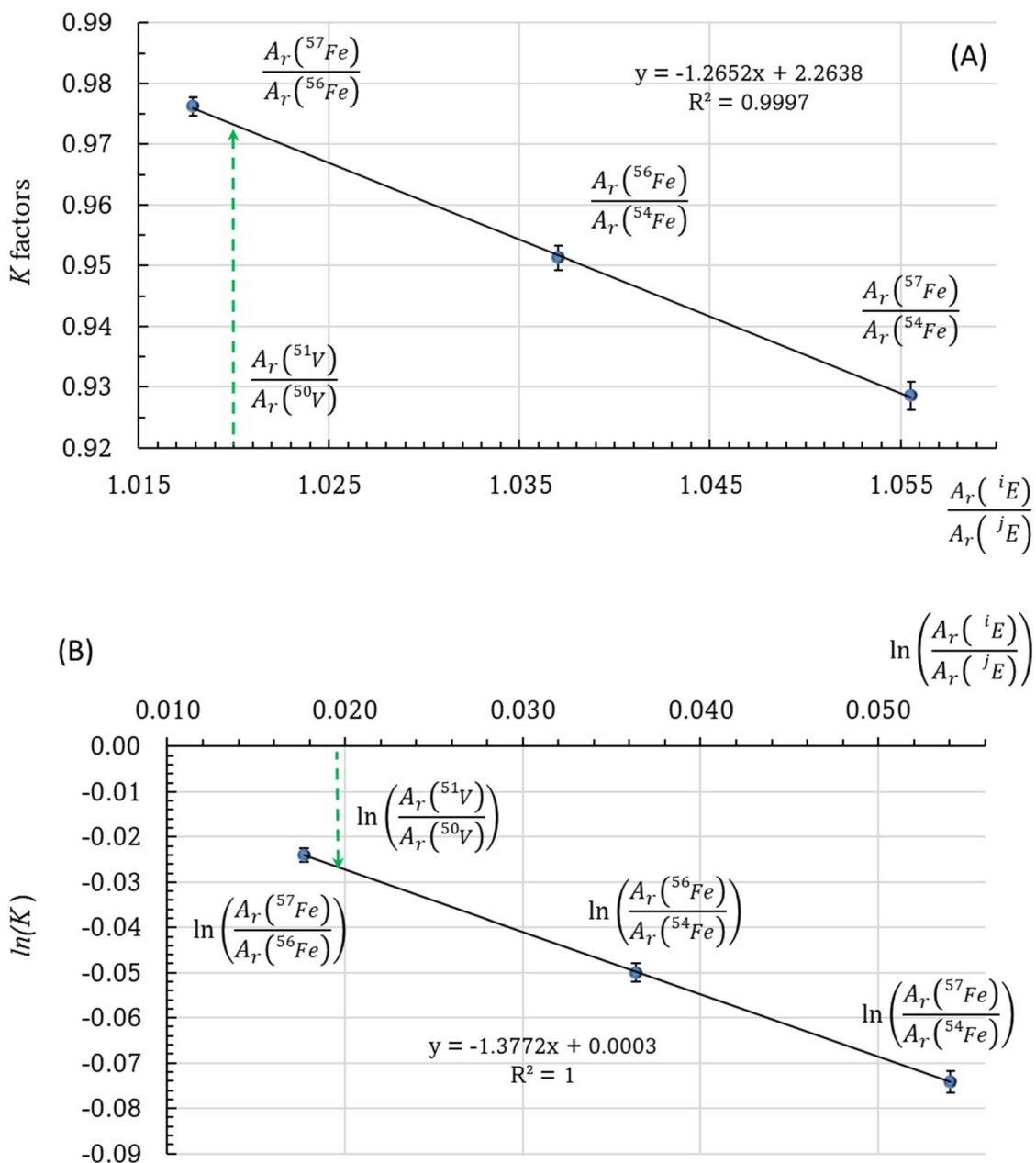


Fig. 5 A relationship between calibration factors obtained for the internal standard (IRMM-014) and the relative atomic mass ratios of ^{54}Fe , ^{56}Fe , and ^{57}Fe isotopes in a typical measurement session plotted: (A) on a linear scale; (B) on a ln–ln scale. It can be seen that the relative atomic mass ratio of vanadium isotopes sits within the range of values defined by Fe isotopes.

Fe isotopes implies mass-dependent instrumental isotope fractionation in the mass spectrometer. As vanadium has only two stable isotopes, there is no way of identifying a potential mass-independent component in instrumental fractionation of vanadium isotopes from measured ratios (a three-isotope plot can be used for this purpose in other elements). Deviations from the mass-dependent distribution in measured isotope ratios can be caused by a spread in the ion energy during transmission of ions in the mass spectrometer.³³ However, measured Fe isotope ratios of the internal standard are consistent with the mass-dependent pattern, ruling out such a spread as the cause. Mass-independent isotope fractionation

can also potentially occur due to the differences in nuclear properties of isotopes. However, a careful examination of research on the topic shows that it is very unlikely that any detectable mass-independent vanadium isotope fractionation can occur during measurements by MC-ICP-MS. Of the two known mechanisms, the nuclear volume effect was predicted to be negligible for naturally occurring vanadium species.⁶ Another mechanism, the magnetic isotope effect, requires a solvent cage to manifest itself.³⁴ Yet it is unrealistic for a solvent cage to be formed in the plasma and the plasma interface region of the ICP-MS.^{34,35}



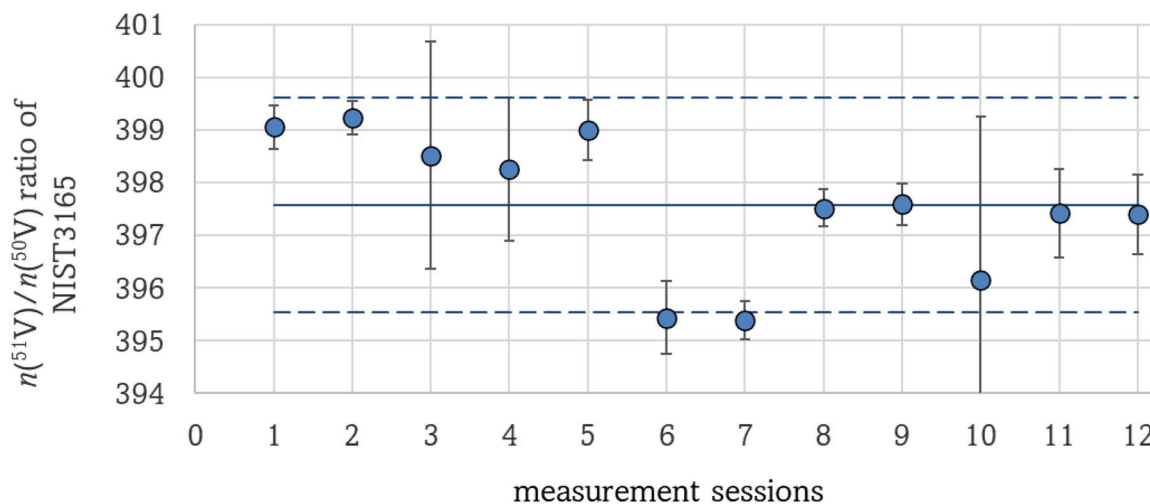


Fig. 6 $n(^{51}\text{V})/n(^{50}\text{V})$ isotope ratios obtained by the new method, with determining K factors for measured $^{51}\text{V}/^{50}\text{V}$ isotope ratios using a function of K factors versus relative atomic mass ratios for three Fe isotopes of the internal standard (see the text for details). Uncertainty bars are combined standard uncertainty. Solid line and dashed lines are the grand mean and expanded uncertainty ($k = 2$) of the results. Mean value is equal to 397.6 ± 2.0 ($U_{\text{expanded}}, k = 2$).

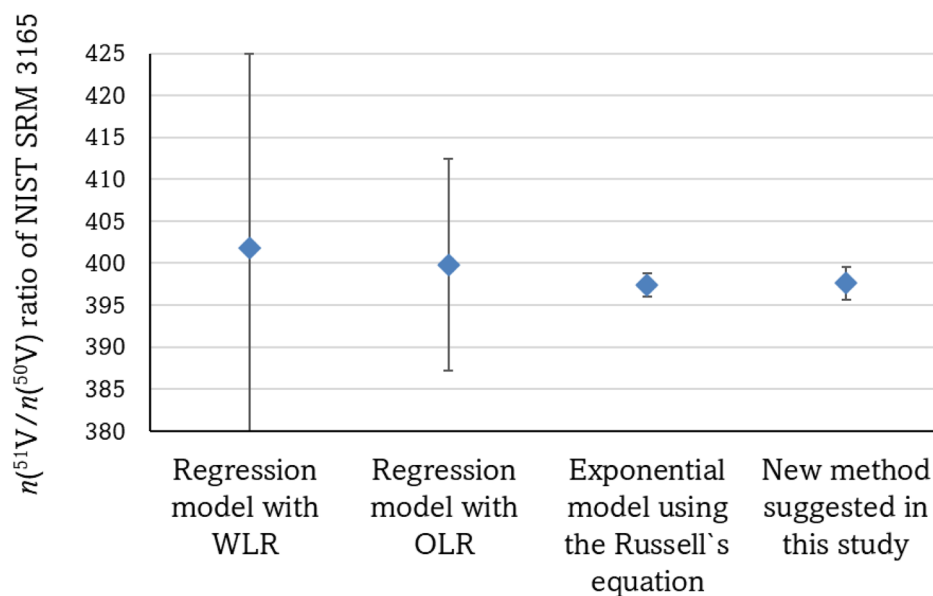


Fig. 7 $n(^{51}\text{V})/n(^{50}\text{V})$ isotope ratios of the NIST SRM 3165 vanadium standard determined by different techniques of internal standardisation. Uncertainty bars are expanded uncertainties ($k = 2$).

The isotope abundances and atomic weight of vanadium in NIST SRM 3165

The atomic weight of an element is the weighted sum of the relative masses of its isotopes, $A_r(^iE)$, and the abundance of each isotope, $x(^iE)$:³⁶

$$A_r(E) = \sum [x(^iE) \cdot A_r(^iE)] \quad (5)$$

The abundances of ^{50}V and ^{51}V isotopes were calculated from the $n(^{51}\text{V})/n(^{50}\text{V})$ isotope ratio, R , obtained for the NIST SRM 3165 standard as follows:

$$x(^{50}\text{V}) = \frac{1}{(R+1)} \quad (6)$$

$$x(^{51}\text{V}) = \frac{R}{(R+1)} \quad (7)$$

By using the exact relative atomic masses of vanadium isotopes,³⁷ we determined the atomic weight of the above standard to be 50.94146 ± 0.00003 ($U_{\text{expanded}}, k = 2$). Compared to the current IUPAC data which have not been updated since 1977, the uncertainty of the atomic weight obtained for a reference sample of vanadium (NIST SRM 3165) has improved by a factor of four (see the SI for details). The abundances of ^{50}V and ^{51}V isotopes in NIST SRM 3165 were calculated to be 0.00251(3) and 0.99749(3), respectively, with the coverage factor $k = 2$.



Conclusions

When assessing the performance of the existing calibration approaches, we observed that the so-called regression model was unable to determine the $n(^{51}\text{V})/n(^{50}\text{V})$ isotope ratios of the NIST SRM 3165 vanadium solution with sufficiently low uncertainty. Difficulties in obtaining accurate and precise parameters of regression seem to be connected with the pattern of measurement data distribution in ln–ln space and the effect of reducing the scatter for large isotope ratios, such as a $^{51}\text{V}/^{50}\text{V}$ ratio of ~ 408 . This observation will need to be considered when the regression model is applied for the determination of large isotope ratios of other elements, e.g., in characterisation of highly enriched isotopic materials.

Interestingly, the exponential model based on the functional form known as the Russell's equation demonstrated reproducible and robust performance, with the grand mean of the mass bias corrected $n(^{51}\text{V})/n(^{50}\text{V})$ isotope ratios of 397.3 ± 1.7 ($U_{\text{expanded}}, k = 2$).

The possibility of using three isotope ratios of the internal standard, $^{56}\text{Fe}/^{54}\text{Fe}$, $^{57}\text{Fe}/^{54}\text{Fe}$, and $^{57}\text{Fe}/^{56}\text{Fe}$, to calibrate the measured $^{51}\text{V}/^{50}\text{V}$ isotope ratio led to the development of a new method based on internal standardisation that does not rely on *a priori* assumed functional form of instrumental isotope fractionation. It involves calculation of a calibration factor for measured vanadium isotopes from a relationship of calibration factors *versus* relative atomic mass ratios obtained for Fe isotope ratios of the internal standard. By using the newly developed method, the $n(^{51}\text{V})/n(^{50}\text{V})$ isotope ratio of the NIST SRM 3165 vanadium solution was determined to be 397.6 ± 2.0 ($U_{\text{expanded}}, k = 2$). This has enabled re-determination of the abundances of ^{50}V and ^{51}V isotopes and the atomic weight of a reference sample of vanadium (NIST SRM 3165), the uncertainties of which have been improved by a factor of four as compared to the last estimate made in 1977. The developed method has good potential for isotopic characterisation of vanadium reference materials.

This work has also highlighted that further improvement in accuracy and precision of $n(^{51}\text{V})/n(^{50}\text{V})$ isotope ratio measurements by internal standardisation can be achieved by using a standard with independently calibrated Fe isotope amount ratios, which is currently unavailable on the market.

Conflicts of interest

There are no conflicts to declare.

Data availability

The data supporting this article have been included as part of the supplementary information (SI). Supplementary information: Table S1 – Isotope ratio data obtained in this study and further experimental details. See DOI: <https://doi.org/10.1039/d5ja00509d>.

Acknowledgements

The work described in this paper was funded in part by the UK Government Department for Science, Innovation & Technology (DSIT) through the National Measurement System Chemical and Biological Metrology Programme and also received funding from the European Partnership on Metrology (Funder ID: 10.13039/100019599, Grant number: 21GRD09 MetroPOEM).

References

- P. I. Premović, I. R. Tonsa, L. López, M. S. Pavlović, O. M. Nešović, S. Lo Monaco, D. M. Đorđević and M. V. Veljković, *J. Inorg. Biochem.*, 2000, **80**, 153–155.
- S. G. Nielsen, J. Prytulak and A. N. Halliday, *Geostand. Geoanal. Res.*, 2011, **35**, 293–306.
- J. Prytulak, S. G. Nielsen, D. A. Ionov, A. N. Halliday, J. Harvey, K. A. Kelley, Y. L. Niu, D. W. Peate, K. Shimizu and K. W. W. Sims, *Earth Planet. Sci. Lett.*, 2013, **365**, 177–189.
- D. Malinovsky and N. Kashulin, *Anal. Methods*, 2016, **8**, 5921–5929.
- M. A. Stow, J. Prytulak, M. C. S. Humphreys, S. J. Hammond and G. M. Nowell, *Earth Planet. Sci. Lett.*, 2024, **643**, 118825.
- T. Fujii, C. Kato, N. Wada, A. Uehara, P. Sossi and F. Moynier, *ACS Earth Space Chem.*, 2023, **7**(4), 912–925.
- L. H. Dong, W. Wei, C. L. Yu, Z. H. Hou, Z. Zeng, T. Chen and F. Huang, *Anal. Chem.*, 2021, **93**(19), 7172–7179.
- W. Yan, B. Zhang, Y. Li, J. Lu, Y. Fei, S. Zhou, H. Dong and F. Huang, *Engineering*, 2025, **46**, 257–266.
- S. Schuth, A. Brüske, S. V. Hohl, S. Y. Jiang, A. K. Meinhardt, D. D. Gregory, S. Viehmann and S. Weyer, *Chem. Geol.*, 2019, **528**, 119261.
- Y. Huang, Z. Long, D. Zhou, L. Wang, P. He, G. Zhang, S. S. Hughes, H. Yu and F. Huang, *Sci. Total Environ.*, 2021, **791**, 148240.
- J. A. J. Watt, I. T. Burke, R. A. Edwards, H. M. Malcolm, W. M. Mayes, J. P. Olszewska, G. Pan, M. C. Graham, K. V. Heal, N. L. Rose, S. D. Turner and B. M. Spears, *Environ. Sci. Technol.*, 2018, **52**, 11973–11974.
- C. Cinder, *Purchase quotation from Oak Ridge National Laboratories*, 2014.
- D. A. Skoog, F. J. Holler and S. R. Crouch, *Principles of Instrumental Analysis*, Cengage Learning, 7th edn, 2018.
- D. T. Burns and M. J. Walker, *Anal. Bioanal. Chem.*, 2019, **411**, 2749–2753.
- J. Meija, L. Yang, R. E. Sturgeon and Z. Mester, *J. Anal. At. Spectrom.*, 2010, **25**, 384–389.
- D. Malinovsky, P. J. H. Dunn and H. Goenaga-Infante, *J. Anal. At. Spectrom.*, 2016, **31**, 1978–1988.
- S. Tong, J. Meija, L. Zhou, B. Methven, Z. Mester and L. Yang, *Anal. Chem.*, 2019, **91**(6), 4164–4171.
- D. C. Baxter, I. Rodushkin and E. Engström, *J. Anal. At. Spectrom.*, 2012, **27**, 1355–1381.
- D. L. MacTaggart and S. O. Farwell, *J. AOAC Int.*, 1992, **75**, 608–614.



- 20 P. Kennedy, *Oxf Bull Econ Stat*, 1983, **45**(4), 389–392.
- 21 W. G. Manning, *J. Health Econ.*, 1998, **17**, 283–295.
- 22 R. Richardson, H. D. Tolley, W. E. Evenson and B. M. Lunt, *PLoS One*, 2018, **13**(5), e0197222.
- 23 Z. Zhu, J. Meija, A. Zheng, Z. Mester and L. Yang, *Anal. Chem.*, 2017, **89**(17), 9375–9382.
- 24 R. Zhang, J. Meija, Y. Huang, X. Pei, Z. Mester and L. Yang, *Anal. Chim. Acta*, 2019, **48**(4), 19–24.
- 25 J. He, J. Meija, X. Hou, C. Zheng, Z. Mester and L. Yang, *Anal. Bioanal. Chem.*, 2020, **412**(24), 6257–6263.
- 26 J. He, L. Yang, X. Hou, Z. Mester and J. Meija, *Anal. Chem.*, 2020, **92**(8), 6103–6110.
- 27 D. Malinovsky, P. J. H. Dunn and H. Goenaga-Infante, *J. Anal. At. Spectrom.*, 2020, **35**, 2723–2731.
- 28 J. Meija, J. He, B. Methven, Z. Mester and L. Yang, *Geostand. Geoanal. Res.*, 2024, **48**(4), 795–805.
- 29 Y. Vander Heyden, A. Nijhuis, J. Smeyers-Verbeke, B. G. M. Vandeginste and D. L. Massart, *J. Pharm. Biomed. Anal.*, 2001, **24**, 723–753.
- 30 W. A. Russell, D. A. Papanastassiou and T. A. Tombrello, *Geochim. Cosmochim. Acta*, 1978, **42**, 1075–1090.
- 31 J. Kragten, *Analyst*, 1994, **119**, 2161–2165.
- 32 P. D. P. Taylor, R. Maeck and P. De Bièvre, *Int. J. Mass Spectrom. Ion Process.*, 1992, **121**, 111–125.
- 33 F. Albarède, P. Telouk, J. Blichert-Toft, M. Boyet, A. Agranier and B. Nelson, *Geochim. Cosmochim. Acta*, 2004, **68**, 2725–2744.
- 34 A. Buchachenko, *J. Phys. Chem. B*, 2013, **117**, 2231–2238.
- 35 D. Malinovsky and F. Vanhaecke, *Anal. Bioanal. Chem.*, 2011, **400**, 1619–1624.
- 36 T. Prohaska, J. Irrgeher, J. Benefield, J. K. Böhlke, L. A. Chesson, T. B. Coplen, T. Ding, P. J. H. Dunn, M. Gröning, N. E. Holden, H. A. J. Meijer, H. Moossen, A. Possolo, Y. Takahashi, J. Vogl, T. Walczyk, J. Wang, M. E. Wieser, S. Yoneda, X.-K. Zhu and J. Meija, *Pure Appl. Chem.*, 2022, **94**(5), 573–600.
- 37 J. R. De Laeter, J. K. Böhlke, P. De Bièvre, H. Hidaka, H. S. Peiser, K. J. R. Rosman and P. D. P. Taylor, *Pure Appl. Chem.*, 2003, **75**, 683–800.

